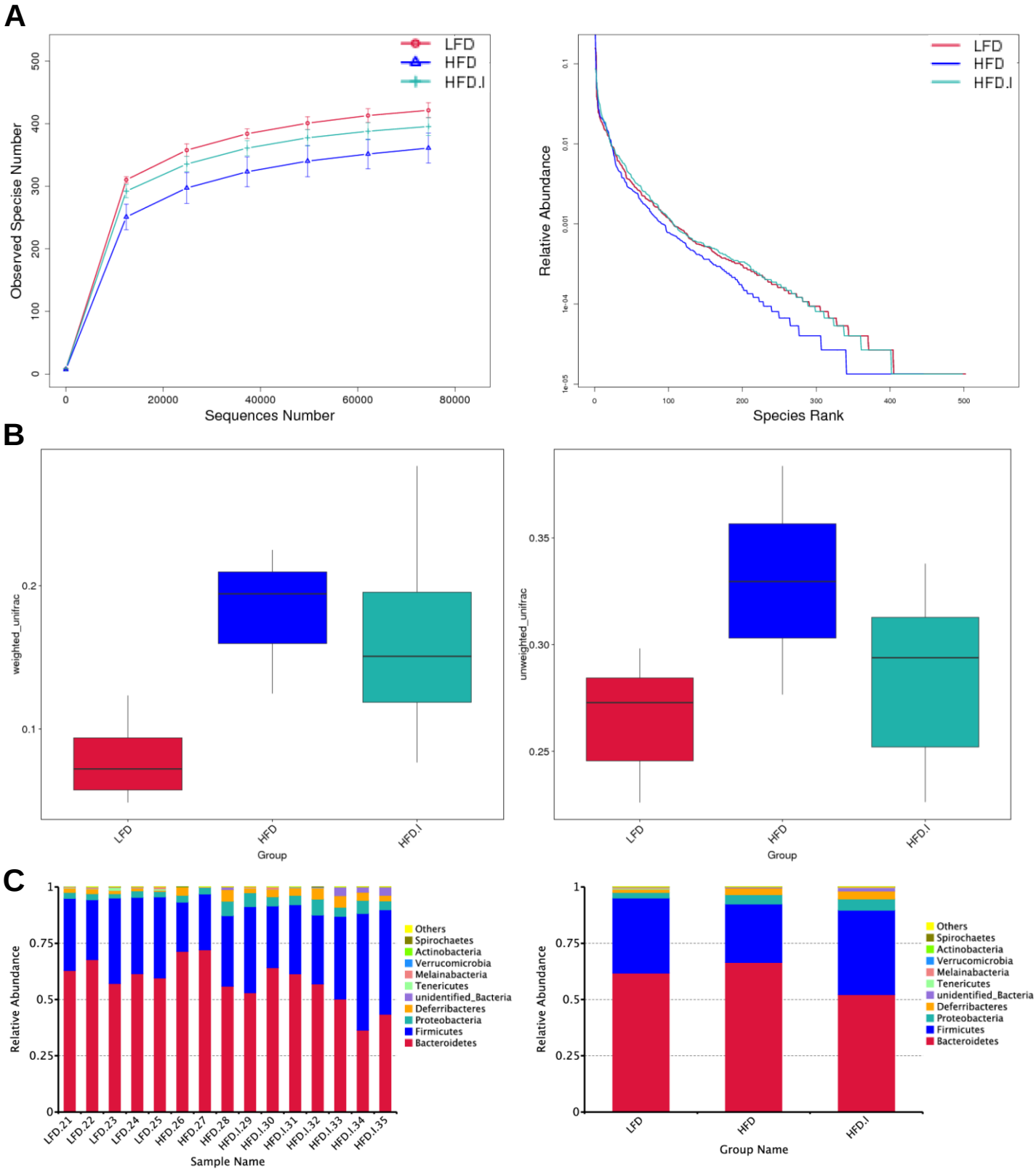

Supplemental Figure S1. Related to Figure 2. Indole alters composition of gut microbiome. Male C57BL/6J mice, at 5 - 6 weeks of age, were fed a low-fat diet (LFD, 10% fat calories) or high-fat diet (HFD, 60% fat calories) for 12 weeks. HFD-fed mice were also daily treated with indole (50 mg/kg, suspension in 5% BSA) or control (Ctrl, 5% BSA) orally for the last 4 weeks of HFD feeding period. After the feeding/treatment period, fecal samples were subjected to analysis of microbiome. (**A**) Indole increases gut microbiome diversity. Left, rarefaction curve; right, rank abundance. (**B**,**C**) Effects of indole on beta diversity (B) and major bacterial phyla (C).

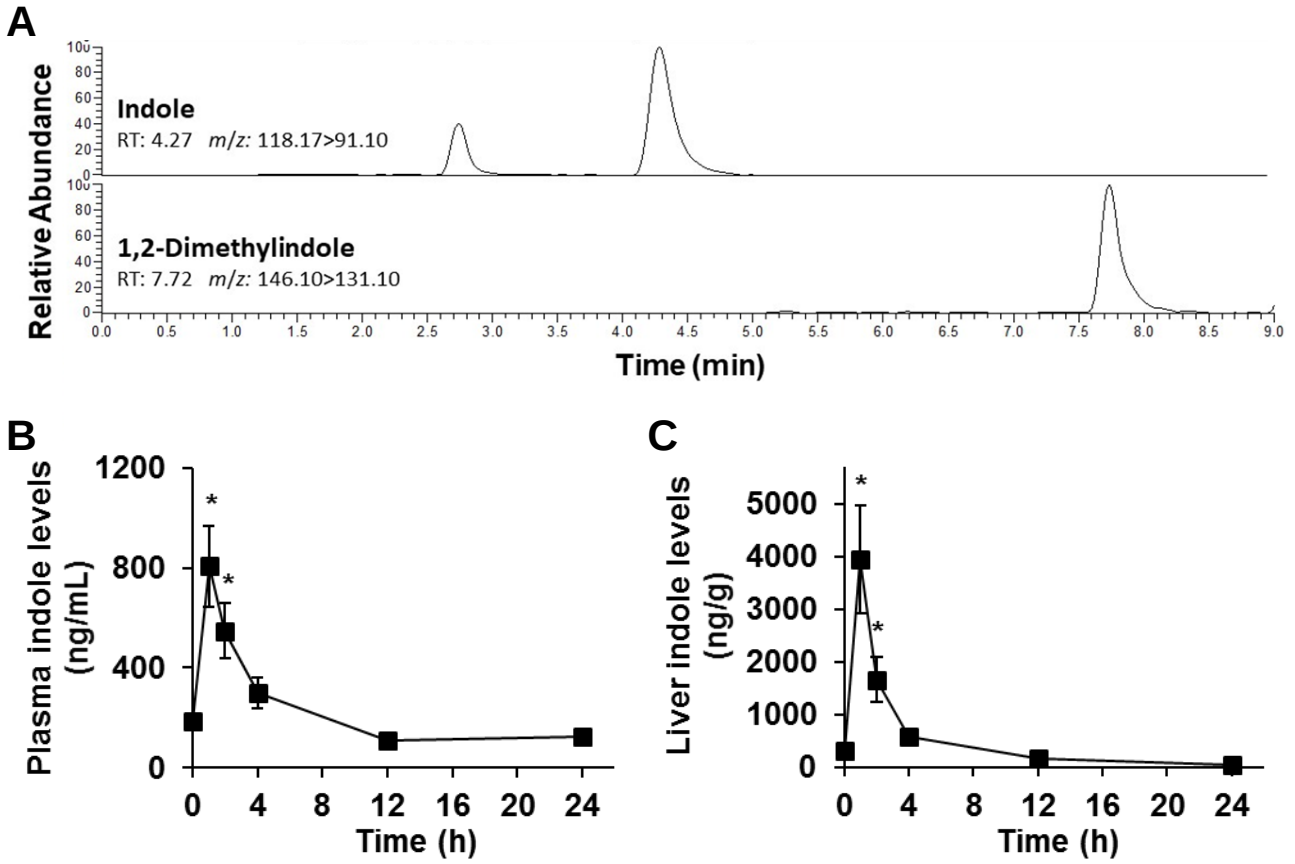

Supplemental Figure S2. Related to Figure 2. Pharmacokinetics of indole.
(**A**) LC/MS/MS spectra of indole and 1,2-dimethylindole that had been added to plasma collected from chow diet-fed C57BL/6J mice. (**B**,**C**) The levels of plasma and liver indole. Male C57BL/6J mice, at 10 - 12 weeks of age, were orally administered a single dose of indole (50 mg/kg). Plasma and/or liver samples were collected prior to oral gavage and/or at the indicated time points post oral gavage, and prepared to measure the levels of indole using LC/MS/MS. For B and C, data are means ± SEM. n = 4 - 8 (plasma) or 3 - 5 (liver). *, $P < 0.05$ the indicated time point vs. 0 time point.

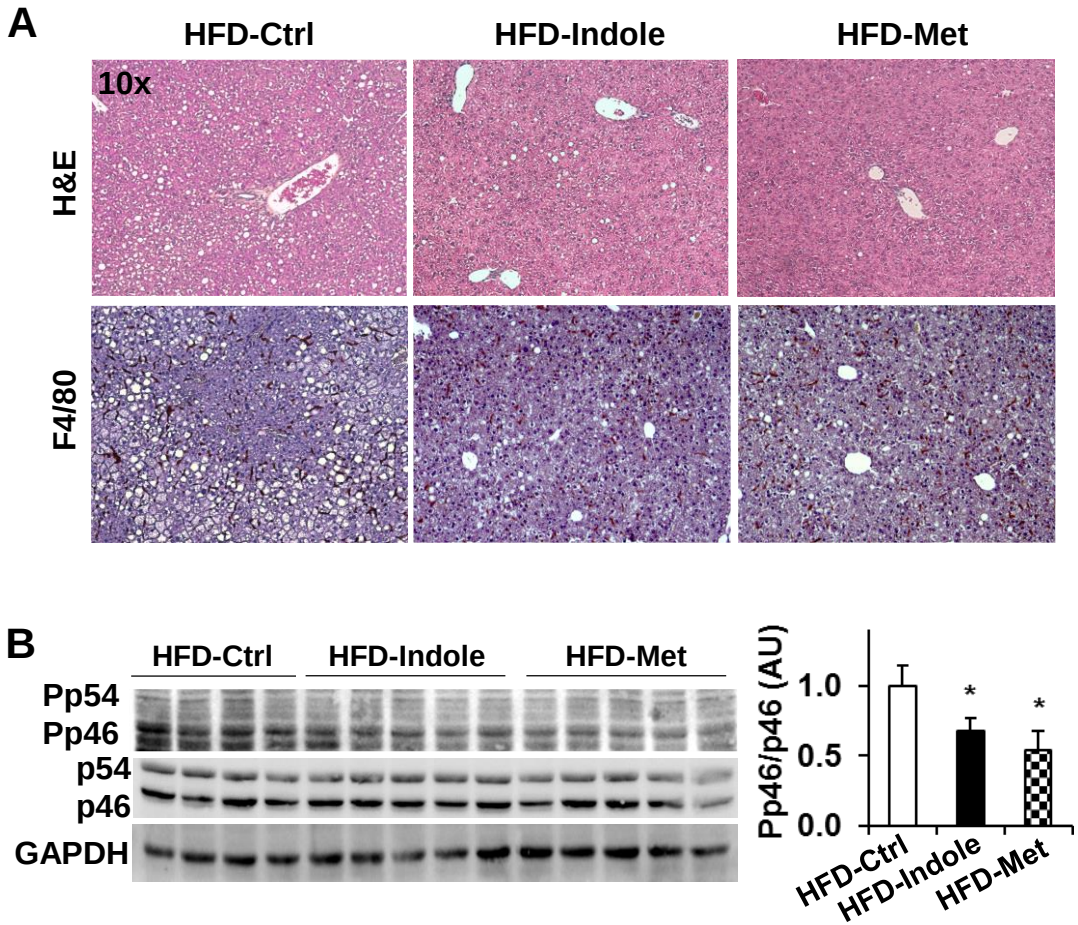

Supplemental Figure S3. Related to Figure 3. Indole treatment alleviates diet-induced NAFLD.

Male C57BL/6J mice, at 5 - 6 weeks of age, were fed an HFD for 12 weeks. HFD-fed mice were also orally treated with indole (50 mg/kg, suspension in 5% BSA), metformin (Met, 150 mg/kg) or control (Ctrl, 5% BSA) daily for the last 4 weeks of HFD feeding period. (**A**) Liver sections were stained with H&E or for F4/80 expression. (**B**) Liver phosphorylation states of JNK p46. Liver lysates were subjected to Western blot analysis. Bar graph, quantification of blots. Data are means ± SEM. n = 4 - 5. *, $P < 0.05$ HFD-Indole or HFD-Met vs. HFD-Ctrl.

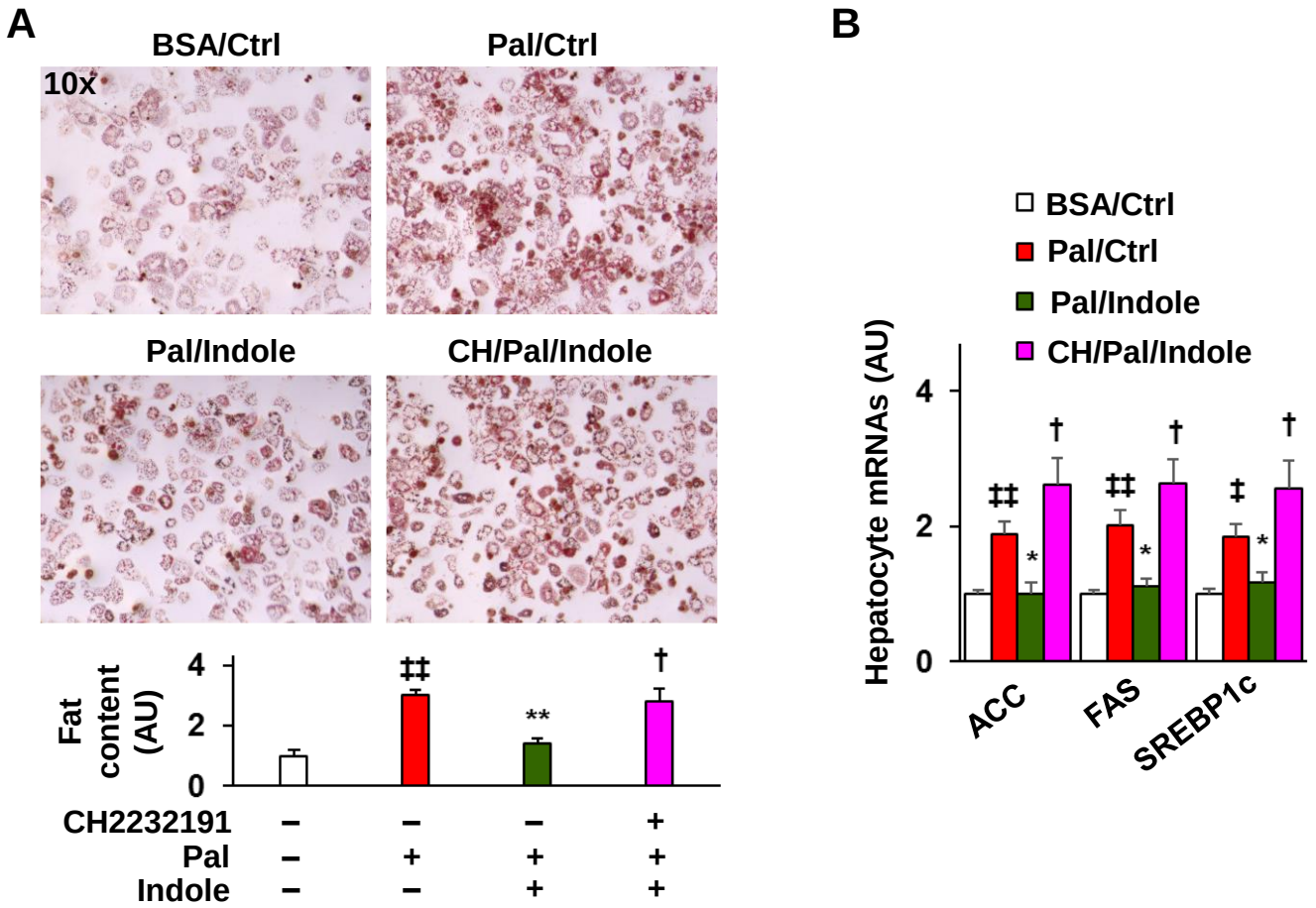

Supplemental Figure S4. Related to Figure 4. Inhibition of AhR impairs the effect of indole on decreasing hepatocyte fat deposition and lipogenic gene expression.

(**A**) Hepatocyte fat deposition. Bar graph, quantification of fat content. (**B**) Hepatocyte expression of genes for lipogenesis. The levels of mRNAs were quantified using real-time PCR. For A and B, primary hepatocytes were pre-treated with AhR inhibitor CH223191 (20 μM) for 10 min and then supplemented with palmitate (Pal) (250 μM, conjugated in 10% bovine serum albumin (BSA)) or BSA in the presence of indole (0.2 mM) or control (Ctrl) for 24 hr. For A, the cells were stained with Oil Red O for 1 hr prior to harvest. For bar graphs in A and B, data are means ± SEM. n = 4 - 6. *, $P < 0.05$ and **, $P < 0.01$ Pal/Indole (presence of Pal and Indole) vs. Pal/Ctrl (presence of Pal) (in A) for the same gene (in B); †, $P < 0.05$ CH/Pal/Indole vs. Pal/Indole (in A) for the same gene (in B); ‡, $P < 0.05$ ‡‡, $P < 0.01$ Pal/Ctrl vs. BSA/Ctrl (absence of CH, Pal, and/or Indole in A) for the same gene (in B).

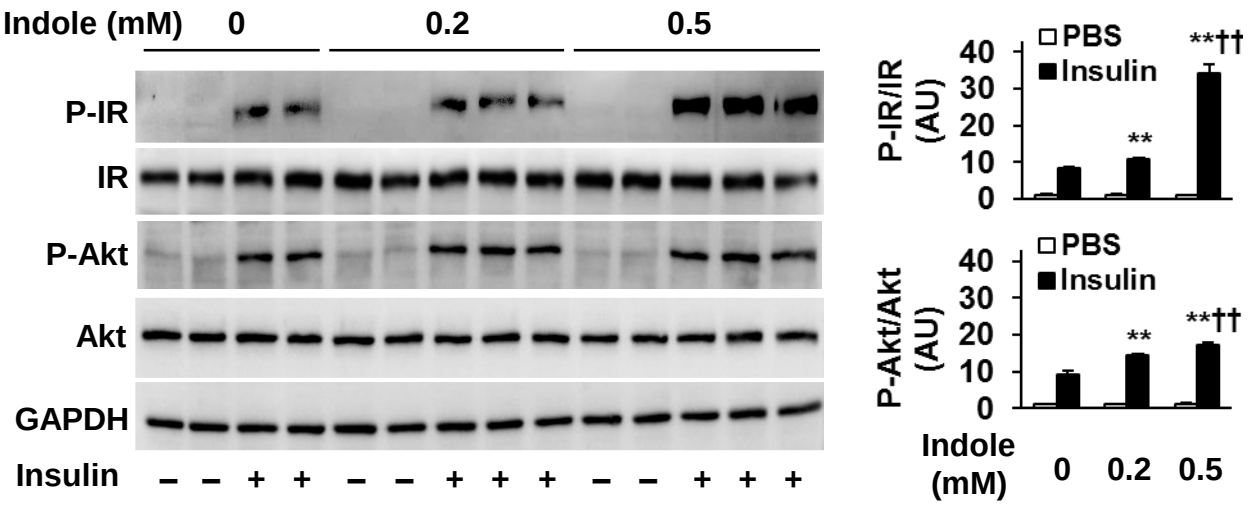

Supplemental Figure S5. Related to Figure 4. Treatment with indole improves hepatocyte insulin signaling.

Primary mouse hepatocytes were treated with indole (0.2 or 0.5 mM) or control (Ctrl) for 24 hr. Prior to harvest, the cells were treated with or without insulin (100 nM) for 30 min. Left panels, cell lysates were subjected to Western blot analysis. Bar graphs, quantification of blots. Data are means ± SEM. n = 4 - 6. **, $P < 0.01$ Indole (0.2 or 0.5) vs Ctrl (in the absence of indole) under insulin-stimulated condition; ††, $P < 0.01$ Indole (0.5) vs. indole (0.2).under insulin-stimulated condition.

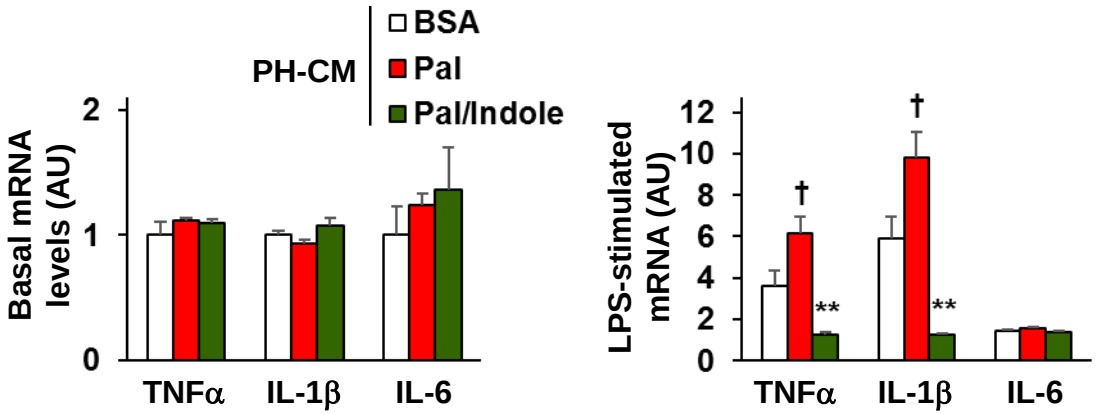

Supplemental Figure S6. Related to Figure 4. Indole-driven hepatocyte factors act to decrease macrophage cytokine expression.

Bone marrow cells were isolated from C57BL/6J mice and differentiated into macrophages (BMDM). After differentiation, BMDM were incubated with media supplemented with conditioned media from primary mouse hepatocytes that were pre-treated with or without indole (0.2 mM) for 24 hr in the presence of palmitate (Pal, 250 μM) or BSA for 24 hr. After initial incubation, the treated primary hepatocytes were maintained in fresh media for an additional 24 h prior to collection of conditioned media (PH-CM). Thereafter, BMDM were incubated with mixture of BMDM media and PH-CM at a 1:1 ratio for 24 hr. Prior to harvest, PH-CM-treated BMDM were treated with LPS (20 ng/mL) for 6 hr. The mRNAs of cytokines were quantified using real-time PCR. Data are means ± SEM. n = 6 - 8. **, $P < 0.01$ Pal/Indole-treated PH-CM vs. Pal-treated PH-CM for the same gene; †, $P < 0.05$ Pal-treated PH-CM vs. BSA-treated PH-CM for the same gene.

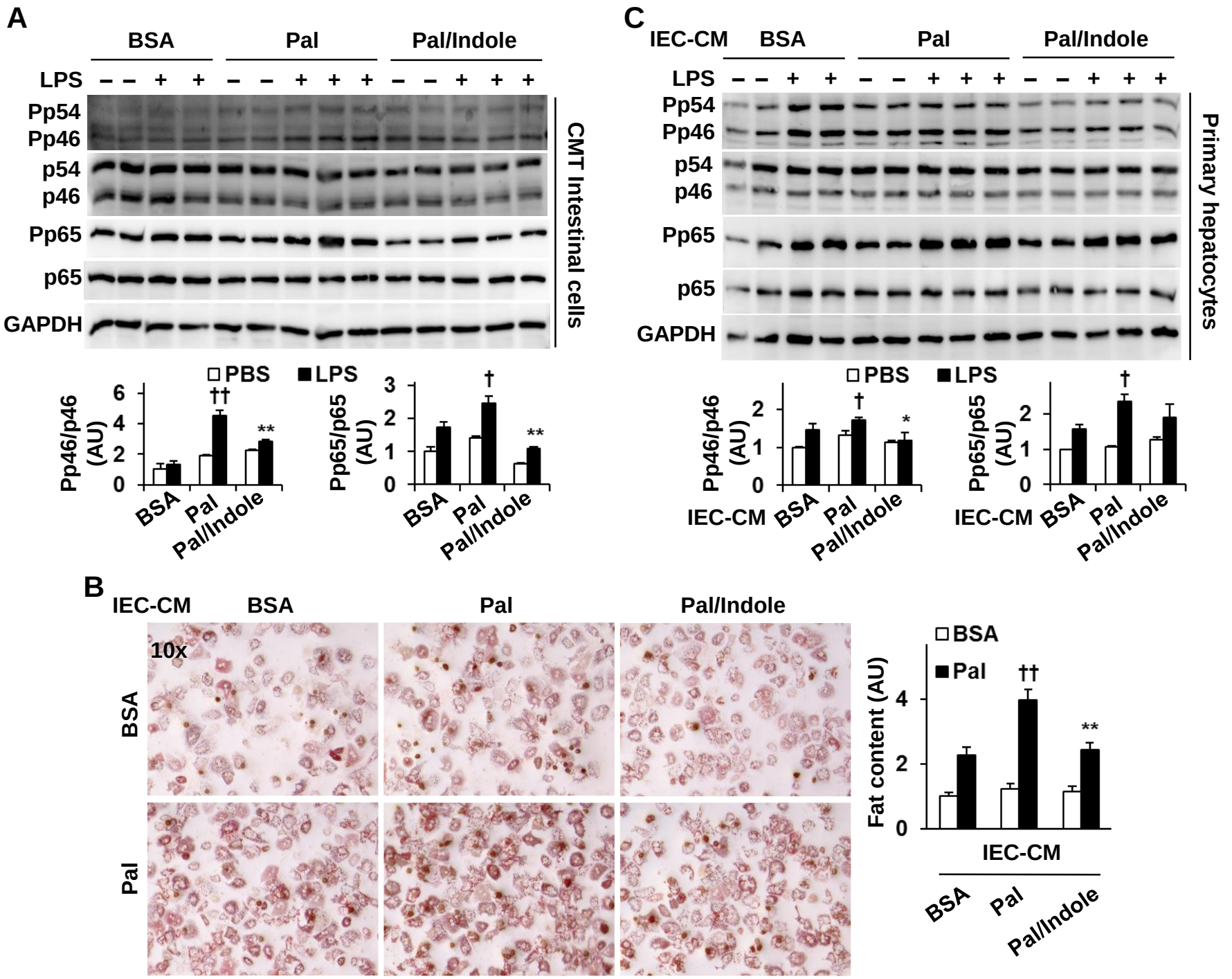
A
BSA
Pal
Pal/Indole
LPS
Pp54
Pp46
p54
p46
Pp65
p65
GAPDH
CMT Intestinal cells
PBS
LPS
Pp46/p46 (AU)
Pp65/p65 (AU)
C
IEC-CM
Primary hepatocytes
B
10x
Fat content (AU)

Supplemental Figure S7. Related to Figure 4. Indole-driven IEC factors act to decrease hepatocyte fat deposition and proinflammatory responses.

(**A**) Proinflammatory responses of intestinal epithelial cells (IEC). CMT-93 cells (a line of IEC) were treated with or without indole (0.2 mM) for 24 hr in the presence of palmitate (Pal, 100 μM) or BSA for 24 hr. After treatment/incubation, the cells were supplemented with fresh media and maintained for an additional 24 hr and harvested for IEC conditioned media (CM) and cell lysates. (**B**,**C**) Effects of IEC-CM on hepatocyte fat deposition (B) and proinflammatory responses (C). Primary mouse hepatocytes were incubated with growth media supplemented with IEC-CM at a 1:1 ratio for 24 hr. For B, IEC-CM-treated hepatocytes were stained with Oil Red O for 1 hr prior to harvest. Bar graph, quantification of fat content. For A and C, the lysates of IEC (A) and IEC-CM-treated hepatocytes (C) were subjected to Western blot analysis. Bar graphs, quantification of blots. For bar graphs in A - C, data are means ± SEM. n = 4 - 6. *, $P < 0.05$ and **, $P < 0.01$ Pal/Indole vs. Pal (in A under LPS-stimulated condition) or Pal/Indole-treated IEC-CM vs. Pal-treated IEC-CM (in B under Pal-stimulated condition and in C under LPS-stimulated condition); †, $P < 0.05$ and ††, $P < 0.01$ Pal vs. BSA (in A under LPS-stimulated condition) or Pal-treated IEC-CM vs. BSA-treated IEC-CM (in B under Pal-stimulated condition and in C under LPS-stimulated condition).

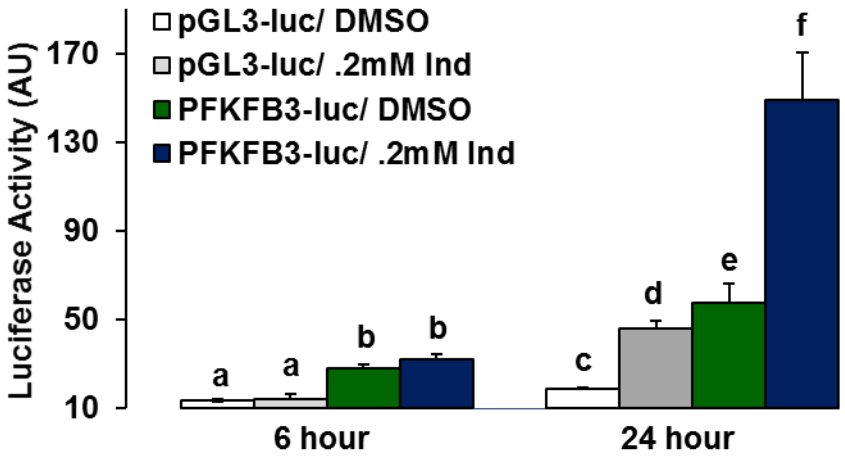

Supplemental Figure S8. Related to Figure 5. Indole stimulates transcription activity of PFKFB3 promoter.

CMT-93 cells, a line of intestinal epithelial cells, were transfected with pGL3-PFKFB3-luc or a control reporter construct (pGL3-luc) for 24 hr and treated with indole (0.2 mM) or DMSO (control) for an additional 6 or 24 hr. Cell lysates were quantified for luciferase activity, which was normalized to protein amount. Data are means ± SEM. n = 6. Differences ($P < 0.05$ or 0.01) were indicated by letters.

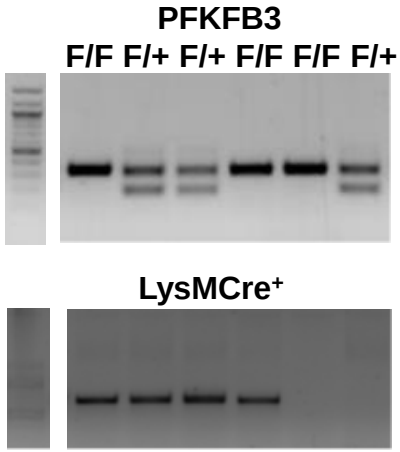

Supplemental Figure S9. Related to Figure 5. Genotyping myeloid cell-specific PFKFB3 knockout mice.

LysMCre^{+}-PFKFB3$^{F/+}$ mice, generated by breeding PFKFB3-floxed ($^{F/F}$) mice with LysMCre^{+} (Mye-PFKFB3$^{+/+}$) mice, were inter-bred to generate homozygous myeloid cell-specific PFKFB3 knockout (LysMCre^{+}-PFKFB3$^{F/F}$ or Mye-PFKFB3$^{-/-}$) mice and heterozygous myeloid cell-specific PFKFB3 knockout (LysMCre^{+}-PFKFB3$^{F/+}$ or Mye-PFKFB3$^{+/-}$) mice.

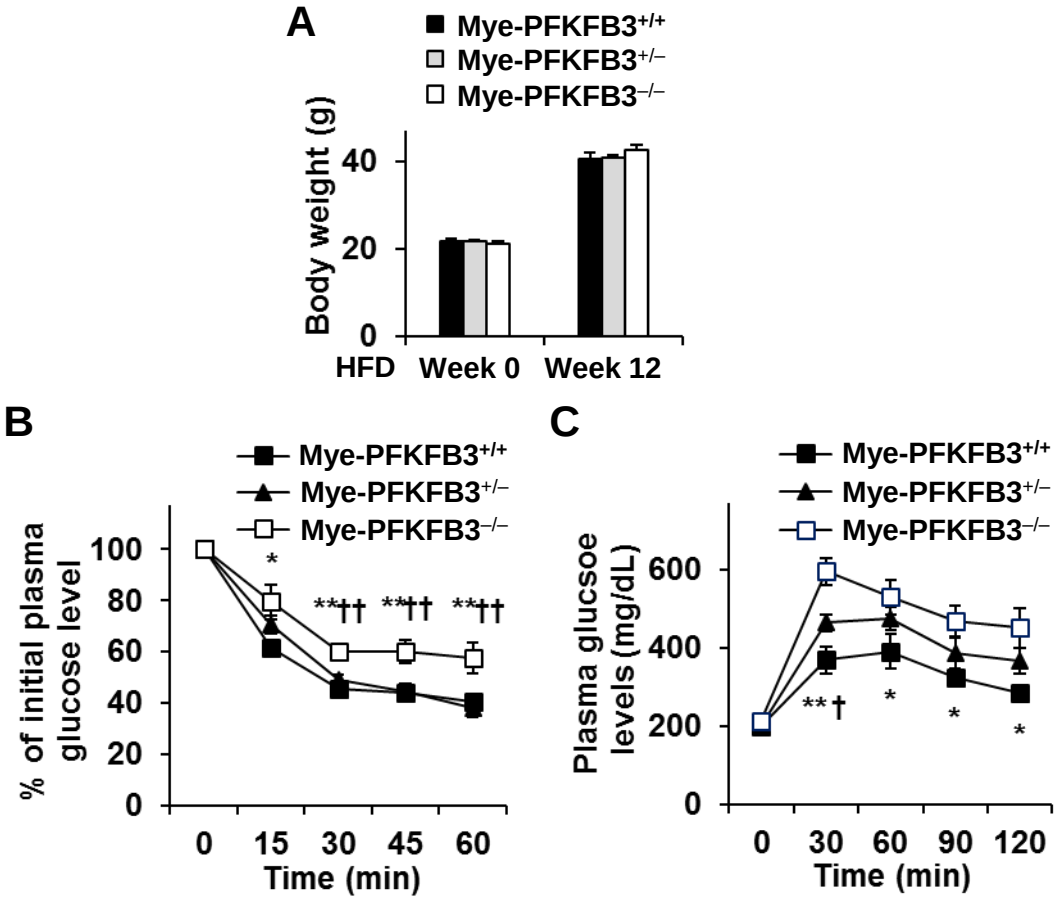

Supplemental Figure S10. Related to Figure 5. Myeloid cell-specific PFKFB3 disruption increases the severity of HFD-induced insulin resistance and glucose intolerance.

Male Mye-PFKFB3$^{-/-}$ mice, Mye-PFKFB3$^{+/-}$ mice, and Mye-PFKFB3$^{+/+}$ littermates, at 5 - 6 weeks of age, were fed an HFD for 12 weeks. (**A**) Body weight was recorded before and after HFD feeding. (**B**,**C**) Insulin (B) and glucose (C) tolerance tests. After the feeding period, mice were given an i.p. injection of insulin (1 U/kg) or glucose (2 g/kg). For A - C, data are means ± SEM, n = 10 - 12. *, $P < 0.05$ and **, $P < 0.01$ Mye-PFKFB3$^{-/-}$ vs. Mye-PFKFB3$^{+/+}$ for the same time point (in B and C). †, $P < 0.05$ and ††, $P < 0.01$ Mye-PFKFB3$^{-/-}$ vs. Mye-PFKFB3$^{+/-}$ for the same time point (in B and C).

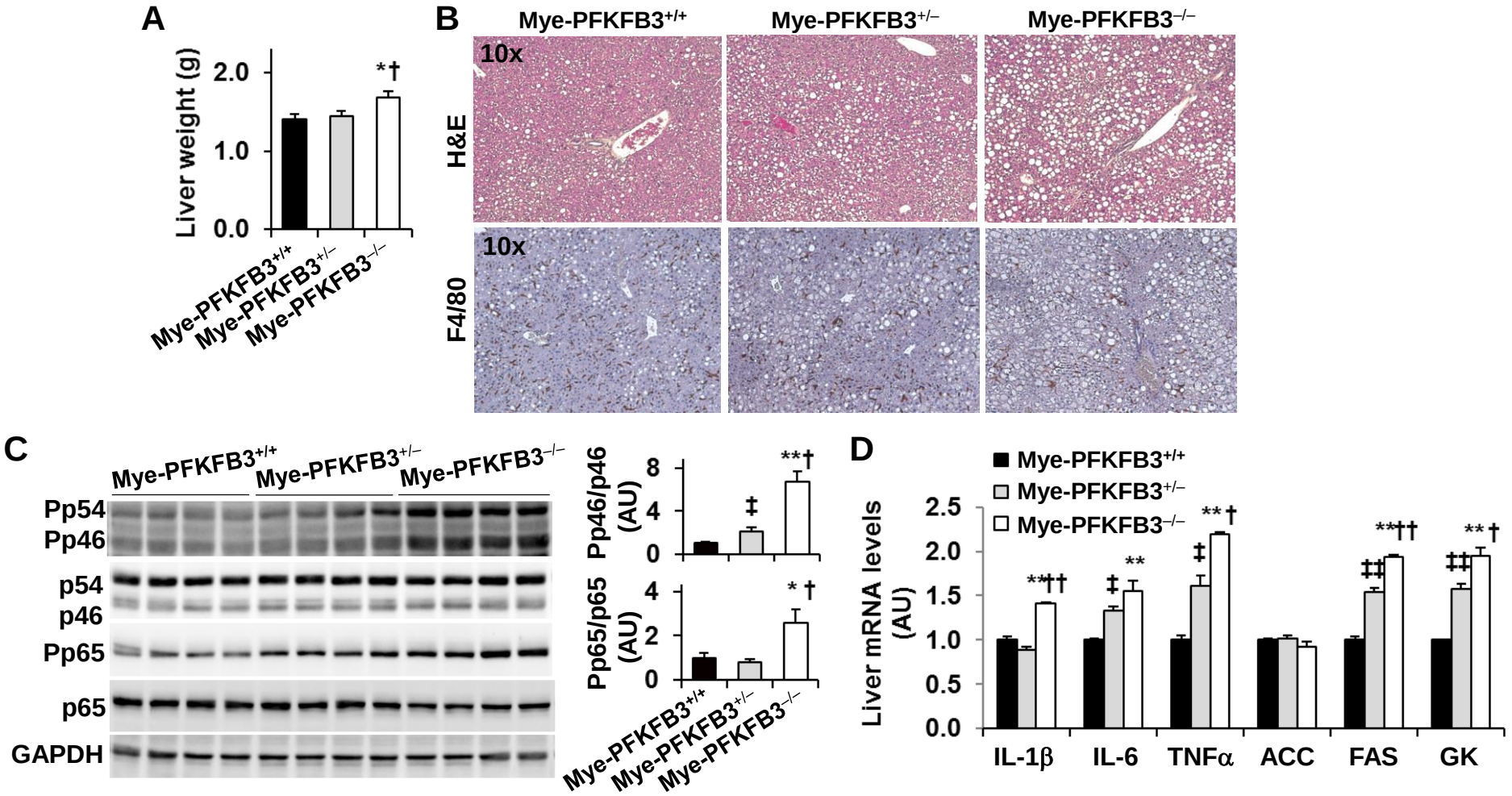

Supplemental Figure S11. Related to Figure 6. Myeloid cell-specific PFKFB3 disruption exacerbates diet-induced NAFLD

Male homozygous myeloid cell-specific PFKFB3 deficient (Mye-PFKFB3$^{-/-}$) mice, heterozygous myeloid cell-specific PFKFB3 disrupted (Mye-PFKFB3$^{+/-}$) mice, and control (Mye-PFKFB3$^{+/+}$) mice, at 5 - 6 weeks of age, were fed an HFD for 12 weeks. (**A**) Liver weight. (**B**) Liver sections were stained with H&E or for F4/80 expression. (**C**) Liver proinflammatory signaling. Left panel, liver lysates were measured for the amount and phosphorylation states of JNK p46 and NFκB p65 using Western blot analysis. Right panels, quantification of blots. (**D**) Liver gene expression was analyzed using real-time RT-PCR. For A, C, and D, numeric data are means ± SEM, n = 10 - 12 (A) or 6 - 8 (C and D). *, $P < 0.05$ and **, $P < 0.01$ Mye-PFKFB3$^{-/-}$ vs. Mye-PFKFB3$^{+/+}$ (in A and C) for the same gene (in D); †, $P < 0.05$ and ††, $P < 0.01$ Mye-PFKFB3$^{-/-}$ vs. Mye-PFKFB3$^{+/-}$ (in A and C) for the same gene (in D); ‡, $P < 0.05$ and ‡‡, $P < 0.01$ Mye-PFKFB3$^{+/-}$ vs. Mye-PFKFB3$^{+/+}$ (in C) for the same gene (in D).

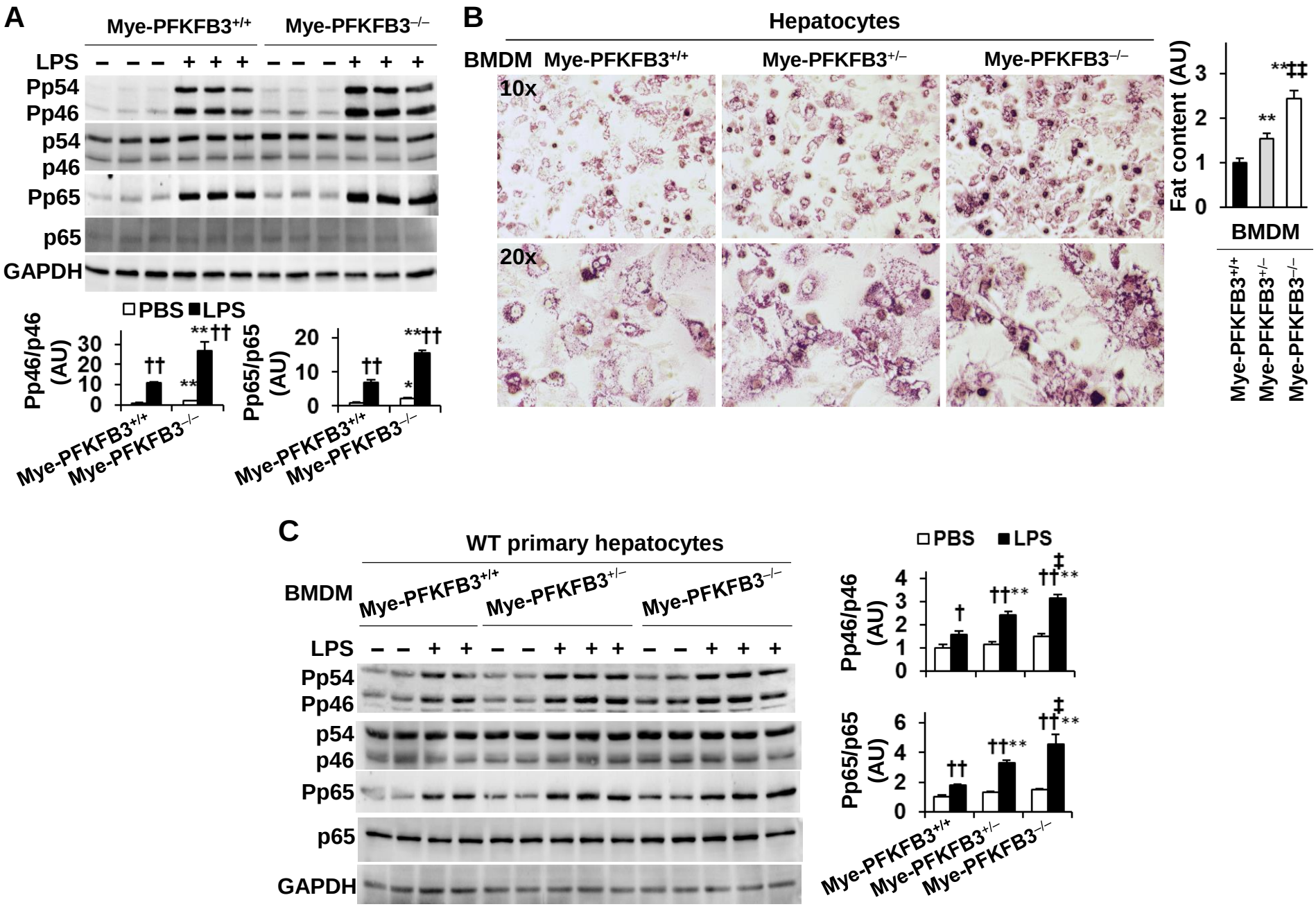
A
Mye-PFKFB3+/+
Mye-PFKFB3−/−
LPS
Pp54
Pp46
p54
p46
Pp65
p65
GAPDH
PBS
LPS
Pp46/p46 (AU)
Pp65/p65 (AU)
Mye-PFKFB3+/+
Mye-PFKFB3−/−
B
Hepatocytes
BMDM
Mye-PFKFB3+/+
Mye-PFKFB3+/−
Mye-PFKFB3−/−
10x
20x
Fat content (AU)
BMDM
C
WT primary hepatocytes
BMDM
Mye-PFKFB3+/+
Mye-PFKFB3+/−
Mye-PFKFB3−/−
LPS
Pp54
Pp46
p54
p46
Pp65
p65
GAPDH
PBS
LPS
Pp46/p46 (AU)
Pp65/p65 (AU)
Mye-PFKFB3+/+
Mye-PFKFB3+/−
Mye-PFKFB3−/−

Supplemental Figure S12. Related to Figure 6. PFKFB3 disruption enhances the effects of macrophages on promoting hepatocyte fat deposition and proinflammatory responses

(**A**) Macrophage proinflammatory signaling. (**B**,**C**) The effects of macrophages on palmitate-induced hepatocyte fat deposition (B) and LPS-stimulated hepatocyte proinflammatory signaling (C). For A - C, BMDM were prepared from male Mye-PFKFB3$^{-/-}$, Mye-PFKFB3$^{+/-}$, and Mye-PFKFB3$^{+/+}$ mice, at 11 - 12 weeks of age. For A, BMDM were treated with or without LPS (100 ng/mL) for 30 min prior to harvest. For B and C, WT primary hepatocytes were co-cultured with BMDM for 48 hr. For B, co-cultures were incubated with palmitate (250 μM) for the last 24 hr and stained with Oil Red O for 1 hr prior to harvest. For C, co-cultures were treated with or without LPS (100 ng/mL) for 30 min prior to harvest. For A and C, cell lysates were subjected to Western blot analysis. Bar graphs, quantification of blots. For A - C, numeric data are means ± SEM, n = 6 - 8. *, $P < 0.05$ and **, $P < 0.01$ Mye-PFKFB3$^{-/-}$ or Mye-PFKFB3$^{+/-}$ vs. Mye-PFKFB3$^{+/+}$ (in B) under the same condition (in A and C); †, $P < 0.05$ and ††, $P < 0.01$ LPS vs. PBS within the same genotype (in A and C); ‡, $P < 0.05$ and ‡‡, $P < 0.01$ Mye-PFKFB3$^{-/-}$ vs. Mye-PFKFB3$^{+/-}$ (in B) under the same condition (in C).

Indole Alleviates Diet-induced Hepatic Steatosis and Inflammation in a Manner Involving Myeloid Cell 6-Phosphofructo-2-Kinase/Fructose-2,6-Biphosphatase 3

Linqiang Ma[1,2,3*], Honggui Li[1*], Jinbo Hu[2*], Juan Zheng[4], Jing Zhou[1], Rachel Botchlett[1], Destiny Matthews[1], Tianshu Zeng[4], Lulu Chen[4], Xiaoqiu Xiao[3], Giri Athrey[5], David W Threadgill[6], Qingsheng Li[7], Shannon Glaser[8], Heather Francis[9], Fanyin Meng[9], Qifu Li[2&], Gianfranco Alpini[9], and Chaodong Wu[1&]

[1] Department of Nutrition, Texas A&M University, College Station, TX 77843, USA,

[2] Department of Endocrinology and [3] the Laboratory of Lipid & Glucose Metabolism, the First Affiliated Hospital of Chongqing Medical University, Chongqing 400016, China;

[4] Union Hospital, Tongji Medical College, Huazhong University of Science and Technology, Wuhan, Hubei 430030, China

[5] Department of Poultry Science, Texas A&M University, College Station, TX 77843, USA

[6] Department of Molecular and Cellular Medicine, College of Medicine, Texas A&M University Health Science Center, College Station, TX 77843, USA,

[7] Nebraska Center for Virology, School of Biological Sciences, University of Nebraska-Lincoln, Lincoln, NE 68588, USA

[8] Texas A&M University College of Medicine, Temple, TX, 76504, USA.

[9] Indiana Center for Liver Research, Richard L. Roudebush VA Medical Center, and Division of Gastroenterology and Hepatology, Department of Medicine, Indiana University School of Medicine, Indianapolis, IN 46202.

*, equal contribution;

& Corresponding addresses:

Chaodong Wu, MD, PhD, College Station, TX 77843, Email: cdwu@tamu.edu, Tel: 001 979 458 1521; or Qifu Li, MD, PhD, Chongqing 400016, China, Email: liqifu@yeah.net, Tel: +8623 8901 1554.

Supplemental Information

MATERIALS AND METHODS

Human subjects and pertinent assays

Subjects who voluntarily provided fasting blood samples and participated in the study were included. Exclusion criteria included: participants diagnosed with diabetes, based on standard oral glucose tolerance tests (according to the World Health Organization 1998 diagnostic criteria) or having a known history of diabetes, age < 20 or > 80 years, a history of inflammatory bowel disease or intestinal resection, current use of probiotics supplements or antibiotic treatment, a malignant tumor, severe cardiovascular diseases, severe liver impairment, or acute infection (white blood cell count $\geq 10 \times 10^9$/L). A total of 137 participants were recruited. The study was approved by the Ethics Committee of the First Affiliated Hospital of Chongqing Medical University. Clinical information regarding past history, family disease history and smoking was collected through interviews. All subjects underwent a physical examination including measurement of weight, height, waist circumference (WC), systolic blood pressure (SBP), and diastolic blood pressure (DBP). Body mass index (BMI) was calculated by dividing weight by the height squared. For assessing general obesity, overweight was diagnosed if 24 $kg/m^2 \leq BMI < 28\ kg/m^2$, obesity was diagnosed if $BMI \geq 28\ kg/m^2$. There were 75, 51, 11 subjects diagnosed as lean, overweight and obesity, respectively. Abdominal obesity was diagnosed WC ≥ 90 cm (for male) or WC ≥ 85 cm (for female), and 57 subjects were diagnosed as abdominal obesity. Liver fat content was assessed by a 64-section multi-detector Computed Tomography (CT) scanner (Lightspeed, GE Healthcare, Milwaukee, WI, USA). The scanning

method was reported previously (1). Mean liver attenuation in an unenhanced CT examination was measured as the CT number (expressed as Hounsfield units), with the use of a technique that containing an ROI placement on a representative portion of the right hepatic lobe. Measurements of splenic attenuation on images were also obtained. Liver fat content was reflected by the mean liver attenuation. Serum indole concentrations were measured by a High Performance Liquid Chromatography (HPLC) method with fluorescence detection established in the Endocrinology Laboratory of Chongqing Medical University (Agilent 1100 HPLC, American). For details, a liquid-liquid extraction was used for serum sample pretreatment. Using an isocratic mixture of 15 mmol/L sodium dihydrogen phosphate solution and methanol (40:60, v/v), chromatographic separation was achieved on a Shim-Pack VP-ODS column (150 mm×4. 6 mm, 4.6 μ m). The fluorescence excitation was 274 nm, with an emission wavelength of 340 nm. The linear range was 2.22 - 88.89 μg/L and the detection limit was 0.11 μg/L for serum indole measurement.

Animal experiments

Wild-type (WT) C57BL/6J mice and LysMCre^{+} mice, in which the expression of Cre recombinase is under the control of Lysosome M promoter, were obtained from Jackson Laboratory (Bar Harbor, ME). PFKFB3-floxed (PFKFB3$^{F/F}$) (C57BL/6 background) mice were generated by Caliper LifeScience (Cyagen US Inc., Santa Clara, CA, USA) and were crossed with LysMCre+ to generate homozygous myeloid cell-specific PFKFB3-disrupted (Mye-PFKFB3$^{-/-}$) mice, heterozygous myeloid cell-specific PFKFB3-disrupted (Mye-PFKFB3$^{+/-}$) mice, and littermate control (Mye-PFKFB3$^{+/+}$) mice. All mice were maintained on 12:12-h light-dark cycles (lights on at 06:00). **Study 1:** Indole pharmacokinetics. Male WT C57BL/6J mice, at 10 - 12 weeks of age, were given a single dose of indole (50 mg/kg, suspension in 5% bovine

serum albumin (BSA)) orally. Prior to oral gavage and at 1, 2, 4, 8, 12, and/or 24 hr post indole oral gavage, plasma and liver samples were collected and quantified for indole levels. **Study 2**: male WT C57BL/6J mice, at 5 - 6 weeks of age, were fed a high-fat diet (HFD, 60% fat calories) for 12 weeks and treated with indole (50 mg/kg/d) or BSA for the last 4 week of feeding period. Additional HFD-fed mice were treated with metformin (150 mg/kg/d) for the last 4 weeks of feeding period. As a control, age- and sex-matched C57BL/6J mice were fed a low-fat diet (LFD, 10% fat calories) for 12 weeks. **Study 3**: male Mye-PFKFB3$^{-/-}$ mice, Mye-PFKFB3$^{+/-}$ mice, and Mye-PFKFB3$^{+/+}$ mice, at 5 - 6 weeks of age, were fed an HFD for 12 weeks as described in Study 2. **Study 4**: male Mye-PFKFB3$^{-/-}$ mice and Mye-PFKFB3$^{+/+}$ mice, at 5 - 6 weeks of age, were fed an HFD for 12 weeks and treated with indole for the last 4 weeks as described in Study 2. LFD and HFD are products of Research Diets, Inc (New Brunswick, NJ). Detailed information of diet composition has been previously described (2) . For **Study 2** through **Study 4**, body weight of the mice was monitored weekly during the feeding period. Also, food amount was recorded weekly and used to calculate food consumption. After the feeding period, some mice in **Study 2** were subjected to collection of intestinal fecal samples for analysis composition of gut microbiome. All other mice in **Study 2** through **Study 4** were fasted for 4 hr before sacrifice for collection of blood and liver samples as described (3-6). Some mice were fasted similarly and used for insulin and glucose tolerance tests as described (3, 4, 7). All study protocols were reviewed and approved by the Institutional Animal Care and Use Committee of Texas A&M University and/or by the Animal Care Committee of Chongqing Medical University.

Analysis of gut microbiome

Fecal samples from LFD-fed mice, HFD-fed mice, and HFD-Indole mice of **Study 2** were analyzed for composition of gut microbiome. In brief, total genomic DNA in the feces was extracted and purified using a commercial kit (QIAGEN, QIAamp Fast DNA Stool Mini Kit, USA). DNA quantity was assessed with agarose gel electrophoresis and spectrophotometry (NanoDrop 2000, Thermo Scientific, USA). A total of 1, 500 ng purified DNA from each sample were used for 16S rDNA sequencing. The 16s rDNA sequencing experiments were carried out by Novogene Bioinformatics Technology Co., Ltd (Beijing, China). Sequencing platform was the Ion S5^{TM}XL platform. The 16S rDNA sequencing data were analyzed in the level of PHYLUM, CLASS, ORDER, FAMILY and GENUS.

Quantification of indole levels in mouse plasma and livers

A total of 100 μL plasma was added to 1, 100 μL of MeOH/H_2O (1:1) with 6 ng/mL 1,2-dimethylindole. After shaking by 250 rpm for 20 min and centrifugation at 12, 000 g for 20 min, a total of 1, 000 μL supernatants was subjected to liquid chromatography - mass spectrometry measurement techniques (UPLC-MS/MS) analysis. Also, a total of 100 mg liver sample was added to 1, 000 μL of sterile water with 60 ng/mL 1,2-dimethylindole internal standards, and homogenized. After centrifugation separation at 12, 000 g for 20 min, a total of 200 μL supernatants was mixed with 1, 100 μL MeOH/H_2O (1:1). After shaking at 250 rpm for 20 min and centrifugation at 12, 000 g for 20 min, a total of 1, 000 μL supernatants was subjected to LC-MS analysis.

Glucose and insulin tolerance tests

Glucose and insulin tolerance tests were performed as previously described (8). Mice were fasted for 4 h and intraperitoneally injected with D-glucose (2 g/kg of body weight) or insulin (1 unit/kg of body weight). For glucose tolerance tests, blood samples (5 μl) were collected from the tail vein before and at 30, 60, 90, and 120 min after the glucose bolus injection. Similarly, for insulin tolerance tests, blood samples were collected from the tail vein before and at 15, 30, 45, 60 min after the bolus insulin injection.

Measurement of plasma parameters

The levels of plasma glucose were measured using a metabolic assay kit (Sigma, St. Louis, MO). The levels of plasma alanine aminotransferase (ALT) were measured using an assay kit (BioVision, Inc. Milpitas, CA).

Histological and immunohistochemical analyses

Paraffin-embedded mouse liver blocks were cut into sections of 5 μm thickness and stained with hematoxylin and eosin (H&E) and/or stained for F4/80 expression with rabbit anti-F4/80 antibodies (1:100) (AbD Serotec, Raleigh, NC) (9, 10).

Cell culture and treatment

Primary hepatocytes were isolated from free-fed WT C57BL/6J mice as described (6). After attachment, hepatocytes were further incubated in M199 supplemented with 10% FBS and 100 U/mL penicillin and 100 μg/mL streptomycin for 24 hr. To examine indole actions on hepatocyte responses, primary mouse hepatocytes were treated with indole (0.2 or 0.5 mM) or control for 24 hr. To examine the proinflammatory responses, indole- or control-treated hepatocytes were

supplemented with LPS (100 ng/mL) for the last 30 min to harvest protein samples or LPS (20 ng/mL) for the last 6 hr to harvest RNA samples. To gain insights for indole regulation of hepatocyte fat deposition, the effect of indole on hepatocyte SREBP1c transcription activity was examined as described below. To examine the involvement of AhR in indole actions, some hepatocytes were pre-treated with AhR inhibitor CH2232191 (20 μM) for 10 min and followed by supplementation with indole (0.2 mM) in the presence of palmitate (250 μM, conjugated in 5% BSA) or BSA for 24 hr. After the treatment/incubation period, hepatocytes were examined for fat deposition and the expression of lipogenic genes. To analyze insulin signaling, some hepatocytes were treated with indole (0.2 mM) for 24 hr. Prior to harvest, the treated cells were supplemented with insulin (100 nM) or control for 30 min. Cell lysates were examined for total protein amount and the phosphorylation states of insulin receptor (IR) and Akt using Western blot analysis. In addition, some hepatocytes were treated with indole (0.2 mM) in the presence of palmitate (250 μM) or BSA for 24 hr, and subjected to incubation with fresh media for an additional 24 hr to collect hepatocyte conditioned media (PH-CM). Some hepatocytes were incubated with mixture of hepatocyte media and conditioned media from intestinal epithelial cells (IEC-CM) (see below) at a 1: 1 ratio for 24 hr, and analyzed for hepatocyte fat deposition and the proinflammatory responses.

RAW264.7 cells were maintained as described (11). At 80% confluence, RAW264.7 cells were treated with indole at 0.2 or 0.5 mM or control for 24 hr and examined for iPFK2 amount. Additional RAW264.7 cells were treated with indole at 0.5 mM for 24 hr and examined for proinflammatory signaling. To study indole regulation of PFKFB3 promoter transcription activity, CMT-93 intestinal cells were subjected to the gene transcription reporter assay as

described below. Bone marrow cells were isolated from the tibias and femurs of male Mye-PFKFB3$^{-/-}$ mice, Mye-PFKFB3$^{+/-}$ mice, and Mye-PFKFB3$^{+/+}$ mice, at 8 -10 weeks of age. After erythrocyte lysis with ammonium chloride (Stem Cell Technologies), bone marrow cells were differentiation with Iscove's modified Dulbecco's medium containing 10% fetal bovine serum and 15% L929 culture supernatant for 8 days to obtain bone marrow-derived macrophages (BMDM) as previously described (12, 13). To examine the proinflammatory responses, indole- or control-treated RAW264.7 cells and differentiated BMDM were supplemented with LPS (100 ng/mL) for the last 30 min to harvest protein samples or LPS (20 ng/mL) for the last 6 hr to harvest RNA samples. Some BMDM were incubated with mixture of macrophage media and PH-CM at a 1:1 ratio for 24 hr and analyzed for the expression of proinflammatory cytokines.

For hepatocyte-macrophage co-culture study, bone marrow cells were prepared from Mye-PFKFB3$^{-/-}$ mice, Mye-PFKFB3$^{+/-}$ mice, and Mye-PFKFB3$^{+/+}$ mice at 6 days prior to hepatocyte isolation. After differentiation, BMDM were trypsinized and added to WT primary mouse hepatocytes at a ratio of 1:10 for 48 hr incubation as described (6, 14). Some hepatocytes were incubated in the absence of macrophages and served as the control. After incubation, co-cultures and control hepatocytes were subjected to assays for fat deposition and the proinflammatory responses.

CMT-93 cells, a line of IEC, were maintained as previously described (15). At 80% confluence, CMT-93 cells were treated with indole (0.2 mM) in the presence of palmitate (100 μM) or BSA for 24 hr, and subjected to incubation with fresh media for an additional 24 hr to

collect IEC-CM and to harvest cell lysates for assessment of proinflammatory signaling using Western blot analysis.

Measurement of hepatocyte fat deposition

To examine hepatocyte fat deposition, indole- or control-treated hepatocytes, as well as hepatocyte-macrophage co-cultures and control primary hepatocytes and IEC-CM-treated hepatocytes, were treated with or without palmitate (250 μM) for 24 hr. At 1 hr prior to harvest, the cells were stained with oil red O and quantified for fat content as described (4, 6).

Biochemical and Molecular assays

To determine inflammatory signaling, lysates of frozen livers or cultured cells were subjected to Western blot analysis to measure total amount and/or phosphorylation states of JNK p46 and NFκB p65 as described (6, 16). To examine insulin signaling, lysates of insulin- or control-treated cells were measured for total amount and the phosphorylation states of insulin receptor and Akt. Similarly, the amount of iPFK2 was examined. GAPDH was used as a loading control. All primary antibodies were from Cell Signaling Technology (Danvers, MA, USA). The maximum intensity of each band was quantified using ImageJ software. Ratios of Pp46/p46 and Pp65/p65, as well as P-IR/IR and P-Akt/Akt, were normalized to GAPDH and adjusted relative to the average of HFD- or PBS-treated Ctrl, HFD-fed Mye-PFKFB3$^{+/+}$, or HFD-fed and control-treated Mye-PFKFB3$^{+/+}$, which was arbitrarily set as 1 (AU). To determine gene expression, the total RNA was isolated from frozen tissues and/or cultured/isolated cells, and subjected to reverse transcription and real-time PCR analysis. Results were normalized to 18s ribosomal RNA and plotted as relative expression to the average of HFD- or PBS-treated Ctrl, PBS-treated

Mye-PFKFB3$^{+/+}$, HFD-fed Mye-PFKFB3$^{+/+}$, or HFD-fed and control-treated Mye-PFKFB3$^{+/+}$, or control cells with or without LPS treatment, which was set as 1.

Gene transcription reporter assay

For hepatocyte study, primary mouse hepatocytes were incubated under nutrient deprivation for overnight and transfected with a plasmid containing firefly luciferase reporter driven by the SRE sequence on FAS gene (pFAS-SRE-luc), or a control plasmid (pGL3-luc) for an additional 24 hr as previously described (6). After transfection, the cells were incubated in the presence or absence of insulin (1 μM) and treated with or without indole (0.5 mM) for an additional 24 hr. After incubation/treatment, the cells were harvested for measurement of luciferase activity. For PFKFB3 promoter study, CMT-93 cells, at 80% confluence, were transfected with each of the three reporter constructs in which luciferase expression was driven by a 6.1 kb fragment of PFKFB3 promoter (pGL3-6.1K), a 3.2 kb irrelevant sequence (pGL3-3.2K), or empty promoter sequence (pGL3) using Lipofectamine Plus (Invitrogen) in DMEM/F12 medium according to the manufacturer's instructions as described before (17). After transection for 24 hr, the cells were also treated with indole (0.2 mM) or control for an additional 24 hr, and harvested for determination of luciferase activity using a Dual Luciferase Reporter Assay System (Promega, Madison, WI).

Statistical Methods

Numeric data are presented as means ± Standard error (SEM). Statistical significance was determined using unpaired, two-tailed ANOVA or Student's *t* tests. Differences were considered significant at the two-tailed $P < 0.05$.

REFERENCES

1. Hahn L, Reeder SB, Muñoz del Rio A, Pickhardt PJ. Longitudinal Changes in Liver Fat Content in Asymptomatic Adults: Hepatic Attenuation on Unenhanced CT as an Imaging Biomarker for Steatosis. AJR. American journal of roentgenology 2015;205:1167-1172.

2. **Luo X**, **Li H**, **Ma L**, Zhou J, Guo X, Woo S-L, Pei Y, et al. Expression of STING is increased in liver tissues from patients with NAFLD and promotes macrophage-mediated hepatic inflammation and fibrosis in mice. Gastroenterology 2018;155:1971-1984.

3. Huo Y, Guo X, Li H, Wang H, Zhang W, Wang Y, Zhou H, et al. Disruption of inducible 6-phosphofructo-2-kinase ameliorates diet-induced adiposity but exacerbates systemic insulin resistance and adipose tissue inflammatory response. J Biol Chem 2010;285:3713-3721.

4. **Huo Y**, **Guo X**, **Li H**, Xu H, Halim V, Zhang W, Wang H, et al. Targeted overexpression of inducible 6-phosphofructo-2-kinase in adipose tissue increases fat deposition but protects against diet-induced insulin resistance and inflammatory responses. J Biol Chem 2012;287:21492-21500.

5. Woo S-L, Xu H, Li H, Zhao Y, Hu X, Zhao J, Guo X, et al. Metformin ameliorates hepatic steatosis and inflammation without altering adipose phenotype in diet-induced obesity. PLoS ONE 2014;9:e91111.

6. **Cai Y**, **Li H**, **Liu M**, Pei Y, Zheng J, Zhou J, Luo X, et al. Disruption of adenosine 2A receptor exacerbates NAFLD through increasing inflammatory responses and SREBP1c activity. Hepatology 2018;68:48-61.

7. **Guo X**, **Li H**, Xu H, Halim V, Zhang W, Wang H, Ong KT, et al. Palmitoleate induces hepatic steatosis but suppresses liver inflammatory response in mice. PLoS ONE 2012;7:e39286.

8. Xu H, Li H, Woo SL, Kim SM, Shende VR, Neuendorff N, Guo X, et al. Myeloid cell-specific disruption of Period1 and Period2 exacerbates diet-induced inflammation and insulin resistance. J Biol Chem 2014;289:16374-16388.

9. Weisberg SP, McCann D, Desai M, Rosenbaum M, Leibel RL, Ferrante AW, Jr. Obesity is associated with macrophage accumulation in adipose tissue. J Clin Invest 2003;112:1796-1808.

10. Wang H, Zhang W, Zhu C, Bucher C, Blazar BR, Zhang C, Chen J-F, et al. Inactivation of the adenosine A2A receptor protects apolipoprotein E-deficient mice from atherosclerosis. Arterioscler Thromb Vasc Biol 2009;29:1046-1052.

11. Mandal P, Pratt BT, Barnes M, McMullen MR, Nagy LE. Molecular mechanism for adiponectin-dependent M2 macrophage polarization: link between the metabolic and innate immune activity of full-length adiponectin. J Biol Chem 2011;286:13460-13469.

12. Odegaard JI, Ricardo-Gonzalez RR, Goforth MH, Morel CR, Subramanian V, Mukundan L, Red Eagle A, et al. Macrophage-specific PPARgamma controls alternative activation and improves insulin resistance. Nature 2007;447:1116-1120.

13. Solinas G, Vilcu C, Neels JG, Bandyopadhyay GK, Luo JL, Naugler W, Grivennikov S, et al. JNK1 in hematopoietically derived cells contributes to diet-induced inflammation and insulin resistance without affecting obesity. Cell Metab 2007;6:386-397.

14. **Odegaard JI**, **Ricardo-Gonzalez RR**, Red Eagle A, Vats D, Morel CR, Goforth MH, Subramanian V, et al. Alternative M2 activation of Kupffer cells by PPARd ameliorates obesity-induced insulin resistance. Cell Metab 2008;7:496-507.

15. Botchlett R, Li H, Guo X, Qi T, Zhao J, Zheng J, Woo S-L, et al. Glucose and palmitate differentially regulate PFKFB3/iPFK2 and inflammatory responses in mouse intestinal epithelial cells. Sci Rep 2016;6:28963.

16. **Guo T**, **Woo S-L**, Guo X, Li H, Zheng J, Botchlett R, Liu M, et al. Berberine ameliorates hepatic steatosis and suppresses liver and adipose tissue inflammation in mice with diet-induced obesity. Sci Rep 2016;6:22612.

17. Chen L, Zhao J, Tang Q, Li H, Zhang C, Yu R, Zhao Y, et al. PFKFB3 control of cancer growth by responding to circadian clock outputs. Sci Rep 2016;6:24324.

Author names in bold designate shared co-first authorship.